J|A|C|S
ARTICLES
Published on Web 03/21/2007

Epitaxial Supramolecular Assembly of Fullerenes Formed by Using a Coronene Template on a Au(111) Surface in Solution

Soichiro Yoshimoto,*[,†,#] Eishi Tsutsumi,[†] Ryuji Narita,[†] Yasujiro Murata,[‡] Michihisa Murata,[‡] Koichi Fujiwara,[‡] Koichi Komatsu,[‡,⊥] Osamu Ito,[§] and Kingo Itaya*[,†]

Contribution from the Department of Applied Chemistry, Graduate School of Engineering, Tohoku University, 6-6-07 Aoba, Sendai 980-8579, Japan, Institute for Chemical Research, Kyoto University, Uji, Kyoto 611-0011, Japan, and Institute of Multidisciplinary Research for Advanced Materials, Tohoku University, Katahira, Aoba-ku, Sendai 980-8577, Japan

Received November 27, 2006; E-mail: so-yoshimoto@aist.go.jp; itaya@atom.che.tohoku.ac.jp

Abstract: Characteristic properties of the coronene layer formed on Au(111) for the epitaxial growth of various fullerenes are described. The electrochemical behavior of the coronene adlayer prepared by immersing a Au(111) substrate into a benzene solution containing coronene was investigated in 0.1 M $HClO_4$. The as-prepared coronene adlayer on Au(111) revealed a well-defined (4×4) structure. Structural changes of the array of coronene molecules induced by potential manipulation were clearly observed by in situ scanning tunneling microscopy (STM). Supramolecularly assembled layers of fullerenes such as C_{60}, C_{70}, $C_{60}-C_{60}$ dumbbell dimer (C_{120}), $C_{60}-C_{70}$ cross-dimer (C_{130}), and C_{60} triangle trimer (C_{180}) were formed on the well-defined coronene adlayer on the Au(111) surface by immersing the coronene-adsorbed Au(111) substrate into benzene solutions containing those molecules. The adlayers thus prepared were characterized by comparison with those which were directly attached to the Au(111) surface. The C_{60} molecules formed a honeycomb array with an internal structure in each C_{60} cage on the coronene adlayer, whereas C_{70} molecules were one-dimensionally arranged with the same orientations. The dimers, C_{120} and C_{130} molecules, formed an identical structure with $c(11 \times 4\sqrt{3})$*rect* symmetry. For the C_{130} cross-dimer molecule, C_{60} and C_{70} cages were clearly recognized at the molecular level. It was difficult to identify the adlayer of the C_{180} molecule directly attached to Au(111); however, individual C_{180} molecules could be recognized on the coronene-modified Au(111) surface. Thus, the adlayer structures of those fullerenes were strongly influenced by the underlying coronene adlayer, suggesting that the insertion of a coronene adlayer plays an important role in the formation of supramolecular assemblies of fullerenes.

Introduction

Supramolecular assemblies on metal surfaces are being explored to control surface properties.[1−4] To fabricate high-quality thin films with superlattices, the two- or three-dimensional construction of such films by epitaxial growth is important in pattern formation at the nanoscale.[5−10] For example, in the construction of organic electronic devices such as field-effect transistors (FETs), the preparation of defect-free crystals

[†] Graduate School of Engineering, Tohoku University.
[‡] Kyoto University.
[§] Institute of Multidisciplinary Research for Advanced Materials, Tohoku University.
[#] Present address: National Institute of Advanced Industrial Science and Technology (AIST), Central 6, 1−1−1 Higashi, Tsukuba, Ibaraki 305-8566, Japan.
[⊥] Present affiliation: Professor Emeritus, Kyoto University, and Professor of Chemistry, Fukui University of Technology.

(1) (a) De Feyter, S.; De Schryver, F. C. *Chem. Soc. Rev.* **2003**, *32*, 139. (b) De Feyter, S.; De Schryver, F. C. *J. Phys. Chem. B* **2005**, *109*, 4290.
(2) (a) Barth, J. V.; Costantini, G.; Kern, K. *Nature* **2005**, *437*, 671 and references therein. For example, (b) Dmitriev, A.; Spillmann, H.; Lin, N.; Barth, J. V.; Kern, K. *Angew. Chem., Int. Ed.* **2003**, *42*, 2670. (c) Stepanow, S.; Lingenfelder, M.; Dmitriev, A.; Spillmann, H.; Delvigne, E.; Lin, N.; Deng, X.; Cai, C.; Barth, J. V.; Kern, K. *Nat. Mater.* **2004**, *3*, 229. (d) Lingenfelder, M. A.; Spillmann, H.; Dmitriev, A.; Stepanow, S.; Lin, N.; Barth, J. V.; Kern, K. *Chem.—Eur. J.* **2004**, *10*, 1913. (e) Stepanow, S.; Lin, N.; Vidal, F.; Landa, A.; Ruben, M.; Barth, J. V.; Kern, K. *Nano Lett.* **2005**, *5*, 901. (f) Classen, T.; Fratesi, G.; Costantini, G.; Fabris, S.; Stadler, F. L.; Kim, C.; de Gironcoli, S.; Baroni, S.; Kern, K. *Angew. Chem., Int. Ed.* **2005**, *44*, 6142. (g) Stepanow, S.; Lin, N.; Barth, J. V.; Kern, K. *Chem. Commun*. **2006**, 2153.
(3) Wan, L.-J. *Acc. Chem. Res.* **2006**, *39*, 334.
(4) Yoshimoto, S. *Bull. Chem. Soc. Jpn.* **2006**, *79*, 1167.
(5) (a) Yokoyama, T.; Yokoyama, S.; Kamikado, T.; Okuno, Y.; Mashiko, S. *Nature* **2001**, *413*, 619. (b) Yokoyama, T.; Kamikado, T.; Yokoyama, S.; Mashiko, S. *J. Chem. Phys.* **2004**, *121*, 11993.
(6) (a) Theobald, J. A.; Oxtoby, N. S.; Phillips, M. A.; Champness, N. R.; Beton, P. H. *Nature* **2003**, *424*, 1029. (b) Theobald, J. A.; Oxtoby, N. S.; Champness, N. R.; Beton, P. H.; Dennis, T. J. S. *Langmuir* **2005**, *21*, 2038. (c) Perdigão, L. M. A.; Perkins, E. W.; Ma, J.; Staniec, P. A.; Rogers, B. L.; Champness, N. R.; Beton, P. H. *J. Phys. Chem. B* **2006**, *110*, 12539.
(7) Griessl, S. J. H.; Lackinger, M.; Jamitzky, F.; Markert, T.; Hietschold, M.; Heckl, W. M. *J. Phys. Chem. B* **2004**, *108*, 11556.
(8) (a) Xu, B.; Tao, C.-G.; Cullen, W. G.; Reutt-Robey, J. E.; Williams, E. D. *Nano Lett.* **2005**, *5*, 2207. (b) Xu, B.; Tao, C.-G.; Williams, E. D.; Reutt-Robey, J. E. *J. Am. Chem. Soc.* **2006**, *128*, 8493.
(9) (a) Bonifazi, D.; Spillmann, H.; Kiebele, A.; de Wild, M.; Seiler, P.; Cheng, F.; Jung, T.; Diederich, F. *Angew. Chem., Int. Ed.* **2004**, *43*, 4759. (b) Spillmann, H.; Kiebele, A.; Stöhr, M.; Jung, T. A.; Bonifazi, D.; Cheng, F.; Diederich, F. *Adv. Mater.* **2006**, *18*, 275. (c) Kiebele, A.; Bonifazi, D.; Cheng, F.; Stöhr, M.; Diederich, F.; Jung, T.; Spillmann, H. *ChemPhysChem* **2006**, *7*, 1462.
(10) (a) Suto, K.; Yoshimoto, S.; Itaya, K. *J. Am. Chem. Soc.* **2003**, *125*, 14976. (b) Yoshimoto, S.; Higa, N.; Itaya, K. *J. Am. Chem. Soc.* **2004**, *126*, 8540. (c) Yoshimoto, S.; Yokoo, N.; Fukuda, T.; Kobayashi, N.; Itaya, K. *Chem. Commun*. **2006**, 500. (d) Suto, K.; Yoshimoto, S.; Itaya, K. *Langmuir* **2006**, *22*, 10766.

 10.1021/ja0684848 CCC: $37.00

is necessary to enhance the mobility of charge carriers in organic crystals. Recently, it was reported that the use of a substrate covered with an atomically flat pentacene monolayer can drastically improve the crystallinity of C_{60} films and increase the field-effect mobility of C_{60} transistors to 2.0−4.9 $cm^2\ V^{-1}\ s^{-1}$, which is a 4- to 5-fold increase over the C_{60} film grown without a pentacene buffer.[11] The insertion of molecular buffered layers of atomically flat pentacene improved the crystallinity of the C_{60} film, suggesting that the insertion of controlled underlying buffered layers can be a general technique for the fabrication of high-performance crystalline plastics and molecular-electronic devices.

Scanning tunneling microscopy (STM) is now well-recognized as an important method for structural investigation of adsorbed layers of molecules on well-defined surfaces in both ultrahigh vacuum (UHV)[1,2,12] and electrolyte solutions.[4,13−15] High-resolution STM made it possible to determine the packing arrangements and even electronic structures of fullerene molecules adsorbed on various surfaces.[12,16,17] The epitaxial thin film of C_{60} on Au(111) was found to take two different structures, $(2\sqrt{3} \times 2\sqrt{3})R30°$ and the so-called "in-phase" (38 × 38), in UHV.[16] Kunitake's group succeeded in preparing a well-ordered C_{60} adlayer on a Au(111) surface in aqueous $HClO_4$ by the transfer of Langmuir (L) films of C_{60} and C_{70} on bare and iodine-modified Au(111) electrodes.[18] They found hexagonal lattices in $HClO_4$, to which the structures of $(2\sqrt{3} \times 2\sqrt{3})R30°$ and (7 × 7) were assigned.[18a] They also succeeded in observing five structural isomers of C_{180} (C_{60} trimers) on Au(111) in solution by using in situ STM.[18d] Subsequently, we reported that C_{60}, C_{120}, and C_{130} adlayers were formed on Au(111) by immersion into benzene solutions containing these molecules.[19]

The formation of mixed molecular adlayers consisting of two or three components has been attempted extensively by using vapor and wet deposition techniques, while STM has been used to understand and design two-dimensional nanoarrays by the bottom-up technology.[1−10] Supramolecular assemblies produced by using the layer-by-layer growth technique have also been investigated to construct molecular architectures. For example, the formation of a two-dimensional nanoporous network using hydrogen bonding[6,7] or metal−organic coordination[2] was reported. Such network arrays could recognize selectively C_{60} or C_{84} molecules as guest molecules. We succeeded in forming a 1:1 supramolecular assembly consisting of fullerenes such as C_{60}, the open-cage C_{60} derivative, and ferrocene-linked C_{60} and metalloporphyrins such as zinc(II) octaethylporphyrin (ZnOEP)[20a−20d] and nickel(II) octaethylporphyrin (NiOEP)[20e] on Au(111) and Au(100) surfaces. Such a supramolecular assembly produced through a donor−acceptor interaction would be useful for the design and organization of functional organic molecules. Furthermore, the formation of homogeneous epitaxial layers was reported for phthalocyanine and porphyrin derivatives on Au(111).[21,22]

For establishing a layer-by-layer method, it is important to understand and to control the first layer, that is, understanding the interaction not only between molecule and substrate but also between the second and the third layers is quite important. As reported in our previous papers, for example, an iodine-modified Au(111) (I−Au(111)) surface plays a role in forming highly ordered arrays of water-soluble organic molecules such as 5,10,15,20-tetrakis(*N*-methylpyridinium-4-yl)porphyrin,[23] crystal violet,[23b] and 4,4′-bis(*N*-methylpyridinium)-*p*-phenylenedivinylene.[23b] Subsequently, the method was extended to the use of a Cl-covered Cu(100) surface on which to form supramolecular layers.[24] These results suggest that a subtle control of interaction between molecule and substrate plays a significant role in the formation of highly ordered molecular arrays. Unfortunately, however, no highly ordered array of C_{60} molecules could be observed because of the high mobility on the I−Au(111) surface.[18b,c] To solve this problem, electron-donating coronene molecules are expected to serve as a buffer layer. As described in our previous papers, coronene molecules form a highly ordered array with (4 × 4) symmetry on Au(111), as characterized by STM[25] and low-energy electron diffraction (LEED).[25b] The adlayer structure of C_{60} on the coronene-modified Au surface is expected to be controlled by donor−acceptor interaction in supramolecular assembly systems because fullerenes are considered to be suitable building blocks for three-dimensional molecular architecture, owing to their strong π-electron accepting ability.[26] Our preliminary result for C_{60} on the coronene-modified Au(111) surface revealed that the coronene layer makes it possible to control surface properties of fullerene assemblies.[27] Recently, Fasel and co-workers reported that a regular nanochain lattice consisting of four or five C_{60} molecules was formed on a high-index plane of Au, a

(11) Itaka, K.; Yamashiro, M.; Yamaguchi, J.; Haemori, M.; Yaginuma, S.; Matsumoto, Y.; Kondo, M.; Koinuma, H. *Adv. Mater.* **2006**, *18*, 1713.
(12) Sakurai, T.; Wang, X. D.; Xue, Q. K.; Hasegawa, Y.; Hashizume, T.; Shinohara, H. *Prog. Surf. Sci.* **1996**, *51*, 263 and references therein.
(13) Gewirth, A. A.; Niece, B. K. *Chem. Rev.* **1997**, *97*, 1129.
(14) Magnussen, O. M. *Chem. Rev.* **2002**, *102*, 672.
(15) (a) Itaya, K. *Prog. Surf. Sci.* **1998**, *58*, 121. (b) Itaya, K. *Electrochemistry* **2001**, *69*, 69. (c) Itaya, K. *Electrochemistry* **2006**, *74*, 19.
(16) (a) Altman, E. I.; Colton, R. J. *Surf. Sci.* **1992**, *279*, 49. (b) Altman, E. I.; Colton, R. J. *Surf. Sci.* **1993**, *295*, 13. (c) Altman, E. I.; Colton, R. J. *Phys. Rev. B* **1993**, *48*, 18244. (d) Altman, E. I.; Colton, R. J. *J. Vac. Sci. Technol., B* **1994**, *12*, 1906.
(17) (a) Gaisch, R.; Berndt, R.; Gimzewski, J. K.; Reihl, B.; Schlitteler, R. R.; Schneider, W. D.; Tschudy, M. *Appl. Phys. A* **1993**, *57*, 207. (b) Gimzewski, J. K.; Modesti, S.; David, T.; Schlittler, R. R. *J. Vac. Sci. Technol., B* **1994**, *12*, 1942.
(18) (a) Uemura, S.; Ohira, A.; Ishizaki, T.; Sakata, M.; Taniguchi, I.; Kunitake, M.; Hirayama, C. *Chem. Lett.* **1999**, 535. (b) Uemura, S.; Ohira, A.; Sakata, M.; Taniguchi, I.; Kunitake, M.; Hirayama, C. *Langmuir* **2001**, *17*, 5. (c) Uemura, S.; Sakata, M.; Hirayama, C.; Kunitake, M. *Langmuir* **2004**, *20*, 9198. (d) Kunitake, M.; Uemura, S.; Ito, O.; Fujiwara, K.; Murata, Y.; Komatsu, K. *Angew. Chem., Int. Ed.* **2002**, *41*, 969.
(19) (a) Yoshimoto, S.; Narita, R.; Tsutsumi, E.; Matsumoto, M.; Itaya, K.; Ito, O.; Fujiwara, K.; Murata, Y.; Komatsu, K. *Langmuir* **2002**, *18*, 8518. (b) Matsumoto, M.; Inukai, J.; Tsutsumi, E.; Yoshimoto, S.; Itaya, K.; Ito, O.; Fujiwara, K.; Murata, M.; Murata, Y.; Komatsu, K. *Langmuir* **2004**, *20*, 1245.
(20) (a) Yoshimoto, S.; Tsutsumi, E.; Honda, Y.; Murata, Y.; Murata, M.; Komatsu, K.; Ito, O.; Itaya, K. *Angew. Chem., Int. Ed.* **2004**, *43*, 3044. (b) Yoshimoto, S.; Tsutsumi, E.; Honda, Y.; Ito, O.; Itaya, K. *Chem. Lett.* **2004**, *33*, 914. (c) Yoshimoto, S.; Saito, A.; Tsutsumi, E.; D'Souza, F.; Ito, O.; Itaya, K. *Langmuir* **2004**, *20*, 11046. (d) Yoshimoto, S.; Honda, Y.; Murata, Y.; Murata, M.; Komatsu, K.; Ito, O.; Itaya, K. *J. Phys. Chem. B* **2005**, *109*, 8547. (e) Yoshimoto, S.; Sugawara, S.; Itaya, K. *Electrochemistry* **2006**, *74*, 175.
(21) Yoshimoto, S.; Tsutsumi, E.; Suto, K.; Honda, Y.; Itaya, K. *Chem. Phys.* **2005**, *319*, 147.
(22) Nishiyama, F.; Yokoyama, T.; Kamikado, T.; Yokoyama, S.; Mashiko, S. *Appl. Phys. Lett.* **2006**, *88*, 253113.
(23) (a) Kunitake, M.; Batina, N.; Itaya, K. *Langmuir* **1995**, *11*, 2337. (b) Batina, N.; Kunitake, M.; Itaya, K. *J. Electroanal. Chem.* **1996**, *405*, 245. (c) Kunitake, M.; Akiba, U.; Batina, N.; Itaya, K. *Langmuir* **1997**, *13*, 1607.
(24) (a) Safarowsky, C.; Merz, L.; Rang, A.; Broekmann, P.; Hermann, B. A.; Schalley, C. A. *Angew. Chem., Int. Ed.* **2004**, *43*, 1291. (b) Safarowsky, C.; Wandelt, K.; Broekmann, P. *Langmuir* **2004**, *20*, 8261.
(25) (a) Yoshimoto, S.; Narita, R.; Itaya, K. *Chem. Lett.* **2002**, 356. (b) Yoshimoto, S.; Narita, R.; Wakisaka, M.; Itaya, K. *J. Electroanal. Chem.* **2002**, *532*, 331.
(26) Billups, W. E., Ciufolini, M. A., Eds. *Buckminsterfullerenes*; VCH: New York, 1993.
(27) Yoshimoto, S.; Tsutsumi, E.; Fujii, O.; Narita, R.; Itaya, K. *Chem. Commun.* **2005**, 1188.

Chart 1. Chemical Structures of Fullerenes, C_{60}, C_{70}, C_{120}, C_{130}, and C_{180}

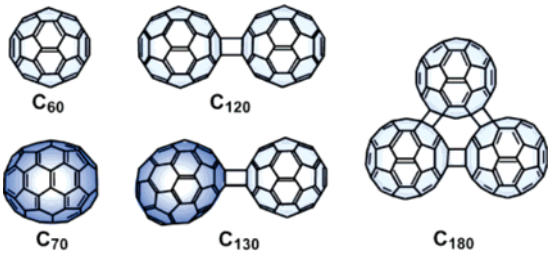

vicinal Au(11 12 12) surface with a {111} microfaceted step.[28] The result indicates that C_{60} molecules as electron acceptors preferentially adsorb at the electron-rich regions near the step edges, leading to the formation of arrays with the perfect periodicity of the Au template. Such a formation of a C_{60} nanochain provides the knowledge for the surface patterning. In contrast, coronene is also one of the promising molecules, as well as pentacene, for the materials of electronic devices such as field-effect transistors and solar cells based on well-ordered organic thin films,[29] as mentioned previously in this paper.[11]

Here, we report on the preparation of epitaxial thin films of fullerene adlayers on coronene-modified Au(111) surfaces. Highly ordered arrays of fullerenes such as C_{60}, C_{70}, $C_{60}-C_{60}$ dumbbell dimer (C_{120}), $C_{60}-C_{70}$ cross-dimer (C_{130}), and C_{60} triangular trimer (C_{180}), as shown in Chart 1, can be constructed as a second layer on the well-defined coronene adlayer on Au(111).

Experimental Section

Coronene (sublimation grade, 99%) was obtained from Aldrich. Fullerenes C_{60} (99.95%) and C_{70} (99.5%) were purchased from MTR Corporation and used without further purification. Fullerene dimer C_{120}, cross-dimer (C_{130}), and triangular trimer (C_{180}) were synthesized by using the high-speed vibration milling technique described in the previous reports.[18d,30] Spectroscopy grade benzene (Kanto Chemical Co.) was used without further purification. An aqueous $HClO_4$ solution was prepared with $HClO_4$ (Cica−Merck) and ultrapure water (Milli-Q SP−TOC; ≥18.2 MΩ·cm).

Au(111) single-crystal electrodes were prepared by the Clavilier method.[31] They were immersed into Milli-Q water saturated with hydrogen quickly after annealing in a hydrogen flame and cooling in the stream of hydrogen.[31] The coronene adlayer was prepared by immersing a Au(111) electrode into a 10 μM benzene solution of coronene for 10 s, as described in our previous papers.[25] The adlayers of C_{60} or C_{70} were prepared by immersing a Au(111) electrode into a ca. 10 μM benzene solution of either C_{60} or C_{70} for 10−20 s, after preparation of the coronene-modified Au(111).[19a] For the preparation of adlayers of C_{120} or C_{130}, a Au(111) electrode was immersed for 3−5 min in a benzene solution saturated with C_{120} or C_{130} after preparing the coronene adlayer on a well-defined Au(111) surface. The fullerene-adsorbed Au(111) electrode was then rinsed with ultrapure water. Both voltammetric and STM measurements were carried out in pure 0.1 M $HClO_4$. In situ STM measurements were performed by using a Nanoscope E (Digital Instruments, Santa Barbara, CA) with a tungsten tip etched in 1 M KOH. To minimize the residual faradaic current, the tips were coated with nail polish. STM images were recorded both in the constant-current mode and in the constant-height mode. All potential values are referred to the reversible hydrogen electrode (RHE) in 0.1 M $HClO_4$.

Results and Discussion

Electrochemical Characterization of the Coronene Adlayer. In the middle portion of Figure 1 are shown typical cyclic voltammograms (CVs) of a clean (black dashed lines) Au(111) electrode and a coronene-modified (red dashed line) Au(111) electrode in 0.1 M $HClO_4$ recorded at the scan rate of 50 mV s^{-1}. The voltammogram for the bare Au(111) electrode indicated by the dotted line in Figure 1 in the double-layer-potential region is identical to that reported previously,[25b] which shows that a well-defined Au(111) surface was exposed to the solution. For the electrode modified with coronene, a small cathodic current peak was observed in the potential range between 0.20 and 0 V.[25b] This peak is assigned to the desorption of coronene molecules from the Au surface. After subsequent immersion of this electrode into a 10 μM benzene solution of C_{60}, the effect of the adsorption of C_{60} was clearly observed in the double-layer charging current. The characteristic peaks of coronene around 0.10 V disappeared, suggesting that the coronene-modified Au(111) was fully covered with C_{60} molecules. Similar CV profiles were obtained with other fullerenes, C_{70}, C_{120}, and C_{130}, on the coronene-modified Au(111) electrode in 0.1 M $HClO_4$.

As reported in our previous papers,[25] a highly ordered (4×4) structure of coronene is formed on Au(111) by simple immersion into a benzene solution containing coronene molecules. In the STM image acquired in a large area of 40×40 nm^2, each coronene molecule can be clearly recognized in the form of a donut ring, as shown in Figure 1a. Each coronene molecule is clearly seen as a hexagon consisting of small spots (see the inset of Figure 1a). The molecular rows consist of bright spots and cross each other at an angle of either 60 or 120° within an experimental error of ±2°. The intermolecular spacing along the <110> direction was estimated to be 1.17 ± 0.03 nm, which corresponds to 4 times the Au lattice constant (4×0.289 nm). The (4×4) symmetry was also confirmed by ex situ LEED measurements in UHV.[25b]

The identical (4×4) structure was consistently observed in the potential range between 1.00 and 0.10 V. When the potential was held within the range of 0.60−0.10 V versus RHE, a partial reconstruction of interfacial gold atoms was found on the Au(111) surface. As can be seen in Figure 1b, reconstructed rows of Au(111) were observed through the molecular layer of coronene. Thus, a stable, well-ordered (4×4) coronene adlayer was observed on both Au(111)−(1×1) and reconstructed Au(111) surfaces in the potential region mentioned earlier in this paper. This is probably due to π-electron donation of coronene to the Au(111) surface, that is, the Au surface becomes negatively charged upon the adsorption of coronene. It is well-known that the surface reconstruction is electrochemically induced at potentials more negative than the potential of zero charge (pzc) to stabilize the first layer of the Au surface.[32] A slightly negative potential manipulation easily induces recon-

(28) Xiao, W.; Ruffieux, P.; Aït-Mansour, K.; Gro1ning, O.; Palotas, K.; Hofer, W. A.; Gro1ning, P.; Fasel, R. *J. Phys. Chem. B* **2006**, *110*, 21394.
(29) Verlaak, S.; Steudel, S.; Heremans, P.; Janssen, D.; Deleuze, M. S. *Phys. Rev. B* **2003**, *68*, 195409.
(30) (a) Wang, G.-W.; Komatsu, K.; Murata, Y.; Shiro, M. *Nature* **1997**, *387*, 583. (b) Komatsu, K.; Wang, G.-W.; Murata, Y.; Tanaka, T.; Fujiwara, K.; Yamamoto, K.; Saunders, M. *J. Org. Chem.* **1998**, *63*, 9358.(c) Komatsu, K.; Fujiwara, K.; Murata, Y. *Chem. Commun.* **2000**, 1583.
(31) Clavilier, J.; Faure, R.; Guinet, G.; Durand, R. J. *J. Electroanal. Chem.* **1980**, *107*, 205.
(32) Dakkouri, A. S.; Kolb, D. M. Reconstruction of Gold Surfaces. In *Interfacial Electrochemistry*; Wieckowski, A., Ed.; Marcel Dekker: New York, 1999; Chapter 10.

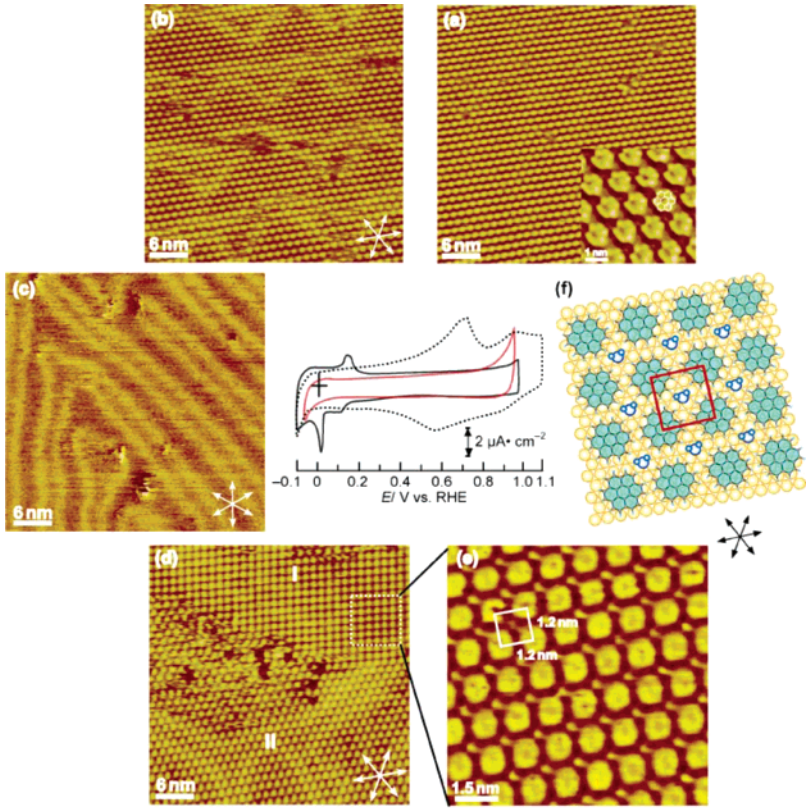

Figure 1. Typical cyclic voltammograms of bare (dotted line), coronene-adsorbed (blue dashed line), and C_{60}/coronene-adsorbed (red solid line) Au(111) electrodes in pure 0.1 M $HClO_4$ recorded at the scan rate of 50 mV s^{-1}. The C_{60} adlayer was formed by immersing coronene-modified Au(111) into a 10 μM C_{60}−benzene solution for 10 s. (a−d) Large-scale (40 × 40 nm^2) STM images of the coronene adlayer on Au(111) observed at (a) 0.75, (b) 0.25, (c) −0.05, and (d) 0.40 V, to which the potential was stepped from 0 V versus RHE. Potentials of the tip and tunneling currents were (a) 0.35 V and 8.60 nA (28.6 nA for the inset), (b) 0.35 V and 3.40 nA, (c) 0.40 V and 1.00 nA, and (d) 0.35 V and 21.5 nA. (e) High-resolution (9 × 9 nm^2) STM image and (f) proposed model of a squarely arranged coronene array in the adlayer on Au(111). The potential of the tip and the tunneling current were 0.15 V and 33.7 nA, respectively. The set of three arrows indicates the close-packed directions of the Au(111) substrate.

struction of the Au surface. Note that the adsorption of coronene on the reconstructed Au(111) surface also revealed the formation of a highly ordered hexagonal array, showing that the coronene adlayer stabilized the reconstructed Au(111) surface. At −0.10 V, the coronene adlayer disappeared, and a reconstructed Au surface was observed at potentials near the H_2 evolution potential because of the high mobility of coronene molecules on the Au surface, as shown in Figure 1c. Furthermore, we performed an in situ observation of the Au(111) surface to investigate the readsorption process of coronene molecules onto the reconstructed Au(111) surface. Upon stepping the potential from a value near the H_2 evolution potential to 0.40 V versus RHE, the readsorption of coronene molecules occurred immediately, and a highly ordered array of coronene molecules was again formed on the reconstructed Au(111) surface. Interestingly, two different phases consisting of square (upper portion; region I) and hexagonal (lower portion; region II) packing arrangements were also found on the reconstructed Au(111) surface in an area of 40 × 40 nm^2, as shown in Figure 1d. At 0.40 V versus RHE, some disordered areas were seen on the terrace, indicating that the readsorption of coronene on the reconstructed Au(111) surface was not complete. A precise comparison of the lattice direction of coronene in the squarely arranged domain with the underlying Au(111) lattice revealed the crossing angle of ca. 3°, suggesting that the relationship between the coronene square lattice and the Au(111) lattice was incommensurate. Details of the squarely packed coronene array in the adlayer are shown in a close-up view of Figure 1e, in which small additional spots are seen in the squarely arranged coronene array, whereas such spots are not seen in the hexagonally arranged domain. We observed such additional spots at tunneling currents higher than 10 nA. The intermolecular distance in the squarely arranged coronene array was found to be ca. 1.2 nm, which is slightly greater than that of the (4 × 4) structure. The molecular rows of coronene were found to cross each other at an angle of ca. 90°. The packing density of the squarely arranged array (θ = 0.058, where θ is the ratio in size of the molecule to the Au atom) on the Au(111) surface was slightly smaller than that of the (4 × 4) structure (θ = 0.0625). It was reported that the structural change of a benzene adlayer on Rh(111) was induced by an applied potential, that is, the adlayer structure of $c(2\sqrt{3} \times 3)rect$ (θ = 0.17) was transformed into the (3 × 3) structure (θ = 0.11) by stepping the potential from 0.35 to 0.25 V versus RHE.[33] The (3 × 3) structure of the benzene adlayer was formed with water molecules on Rh(111) at 0.25 V versus RHE in 0.01 M HF.[31] In analogy, the additional small spots seen in Figure 1e may be assigned to water molecules or hydronium cations. Although the precise adsorption site of each coronene molecule could not be determined, a structural model was prepared for a squarely arranged coronene array, and it is shown in Figure 1f. Such a coadsorption of solvent was reported by Hipps's group

(33) Yau, S.-L.; Kim, Y.-G.; Itaya, K. *J. Am. Chem. Soc.* **1996**, *118*, 7795.

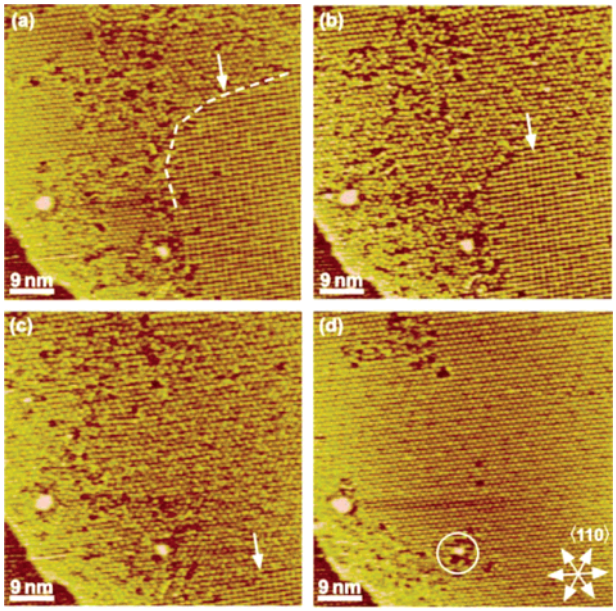

Figure 2. Time-dependent, large-scale STM image (60 × 60 nm^2) of the coronene adlayer on a Au(111) surface in 0.1 M $HClO_4$ obtained at 0.75 V, to which the potential was stepped from 0.40 V versus RHE. Panels (b), (c), and (d) were taken, respectively, 1, 2, and 12 min after panel (a) was recorded. The potential of the tip and the tunneling current were 0.35 V and 1.90 nA, respectively. All STM images were recorded at a scan rate of 7.4 Hz. The set of three arrows indicates the lattice directions of the Au(111) substrate.

for the coronene array on Au(111) in nonconductive solvents such as propionic acid.[34]

When the electrode potential was held at a value more positive than 0.60 V versus RHE, some clusters were formed on the ordered array with lifting of reconstruction. Because the transformation of square symmetry into (4 × 4) symmetry with time was observed, time-dependent, in situ STM observations were performed to investigate the dynamics of phase transition at 0.75 V versus RHE. Figure 2 shows four time-dependent, in situ STM images obtained at the same location (60 × 60 nm^2). In Figure 2a, the white arrow indicates a phase boundary between squarely and hexagonally arranged coronene domains. A squarely arranged coronene domain is seen on the terrace in the right half of this image. Figure 2b shows the STM image obtained 1 min after the image in Figure 2a was recorded. As indicated by the arrow, the domain size of the squarely arranged coronene array in Figure 2b is smaller than that in Figure 2a. A hexagonal region with some defects in the domain was observed in the middle portion of Figure 2b. The STM image taken an additional minute after recording Figure 2b is presented in Figure 2c, which shows that the squarely arranged region became smaller and the hexagonally arranged region extended over almost the entire scanned area. However, the entire area of the hexagonally arranged domain appears to be rough, suggesting that the re-formation of the close-packed (4 × 4) structure was not yet completed at this stage. The STM image obtained 10 min after Figure 2c was recorded is shown in Figure 2d. A smooth and complete hexagonal domain was again formed on the terrace. It is noteworthy that the cluster size on the terrace appearing in the lower part of the STM image of Figure 2d (marked by the white circle) became smaller with time compared

(34) Gyarfas, B. J.; Wiggins, B.; Zosel, M.; Hipps, K. W. *Langmuir* **2005**, *21*, 919.

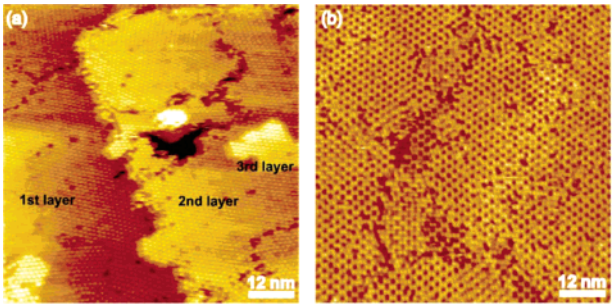

Figure 3. Typical large-scale (75 × 75 nm^2) STM images, acquired at 0.79 V versus RHE, of C_{60} adlayers on (a) a clean Au(111) surface and (b) a coronene-modified Au(111) surface in 0.1 M $HClO_4$. The potential of the tip and the tunneling currents were (a) 0.40 V versus RHE and 1.50 nA and (b) 0.35 V versus RHE and 0.85 nA.

to that of Figure 2a. The increase in surface coverage due to the phase transition from the square to hexagonal packing arrangement was caused by the supply of coronene molecules from these clusters, indicating that these clusters were formed by the excess coronene molecules produced when the coronene adlayer was re-formed on the Au(111) surface. After more than 30 min, the smooth domain composed of hexagonally arranged coronene molecules was completely formed on the terrace, and the clusters diffused and finally disappeared. Thus, the potential-induced structural change of the coronene adlayer on Au(111) is electrochemically reversible. The appearance of the squarely arranged coronene array by electrochemical control is, therefore, attributed to its adlayer structure being metastable.

C_{60} and C_{70} Arrays. Figure 3 shows a typical STM image of a C_{60} adlayer formed on a clean Au(111) surface and that of a well-ordered (4 × 4) coronene adlayer on a Au(111) surface produced by immersion into a ca. 10 μM C_{60}−benzene solution for 10−20 s. It is well-known that the epitaxial film of C_{60} on Au(111) forms hexagonally close-packed ($2\sqrt{3} \times 2\sqrt{3}$)$R$30° and (38 × 38) structures, both in UHV[16] and in solution.[18,19] As shown in Figure 3a, a prolonged immersion caused the multilayer formation of C_{60} with several ordered domains on Au(111), that is, more than three layers were found on the terrace. The difference in height between the first and the second layers was measured to be approximately 0.60 nm, which indicates that the step in the middle of the STM image of Figure 3a is not an atomic step of Au (0.22−0.24 nm) but a step due to the epitaxial layer of C_{60}. Although the high-resolution STM image is not shown here, C_{60} molecules were found to form a ($2\sqrt{3} \times 2\sqrt{3}$)$R$30° or an "in-phase" (38 × 38) structure with an intermolecular distance of 1.0 nm. On the other hand, the C_{60} assembly as the second layer was strongly influenced by the existence of a (4 × 4) coronene adlayer on Au(111), as reported in our previous papers.[27] The STM image shown in Figure 3b is totally different from that of C_{60} directly attached to the Au(111) surface, that is, the honeycomb-like structure was found in the entire scanned area. The result suggests that the coronene adlayer was not replaced by C_{60}. It is known that the C_{60} supramolecular assembly is strongly influenced by the underlying layers of organic molecules such as perylene[27] and porphyrins.[9,20]

To understand the formation process of the interesting C_{60} honeycomb array more precisely, the immersion time dependence of the C_{60} adlayer structure was investigated on the coronene-modified Au(111) surface. When the coverage was low (immersion time shorter than 3 s), both coronene and C_{60}

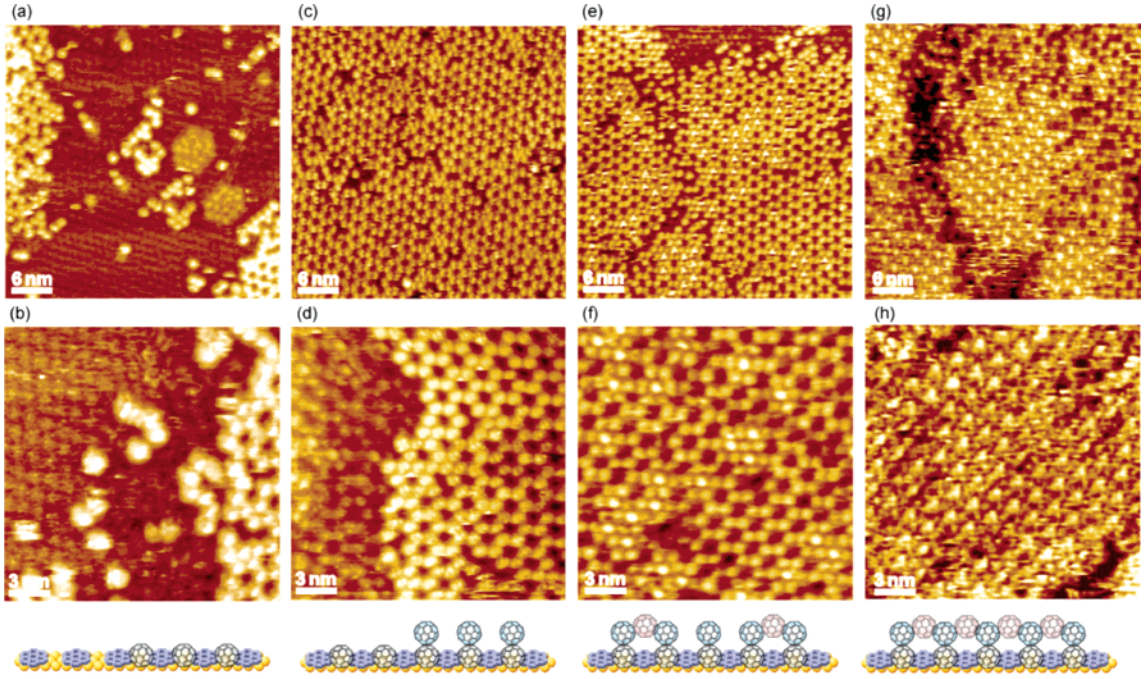

Figure 4. Typical STM images, obtained at 0.85 V for (a) and (b), 0.82 V for (c), (g), and (h), and 0.79 V versus RHE for (d)−(f), of C_{60} honeycomb arrays on a coronene-modified Au(111) surface in 0.1 M $HClO_4$. The potentials of the tip and the tunneling currents were (a) 0.35 V and 0.28 nA, (b) 0.35 V and 0.23 nA, (c) 0.44 V and 0.50 nA, (d) 0.35 V and 0.85 nA, (e) 0.35 V and 0.85 nA, (f) 0.20 V and 0.68 nA, (g) 0.44 V and 0.40 nA, and (h) 0.44 V and 0.50 nA. Schematic illustration of the formation process of the C_{60} honeycomb arrays is shown at the bottom.

layers were observed (see Figure 4a and b). In Figure 4a, both coronene and small C_{60} honeycomb arrays are recognized on the terrace under this modification condition. Molecular rows of coronene are easily seen as hexagonally arranged dark spots. However, a careful inspection revealed that the molecular rows of coronene partially crossed each other at an angle of 3−5°. A close-up view is shown in Figure 4b. Although individual coronene molecules are not clearly distinguishable, it is seen that the directions of cavities consisting of C_{60} molecules are almost in alignment with the molecular rows of the coronene array. Each C_{60} molecule is positioned between molecular rows of coronene. The coronene adlattice was slightly distorted after the adsorption of C_{60}, that is, the intermolecular distance became slightly longer, 1.30 nm. This might have been caused by a change in the structure of the coronene adlayer during the C_{60} modification. According to the report on the adlayer of coronene prepared in UHV, two adlayer structures of coronene, that is, the initial structure with (4.3 × 4.3) symmetry and the final structure with (4 × 4) symmetry, are formed on Au(111).[35] Thus, the existence of a distorted coronene adlattice is consistent with what is reported in the literature.[35] Such a relaxation of the coronene adlattice might make the specific adsorption responsible for the formation of a C_{60} honeycomb array.

When the modification was carried out on the coronene-modified Au(111) surface for 8−10 s, the terrace was entirely covered with a C_{60} honeycomb array, as shown in Figure 4c. A high-resolution STM image is shown in Figure 4d. Fortunately, we could find a step line of the C_{60} honeycomb array. The left portion of the image corresponds to the lower layer of the C_{60} honeycomb array, whereas the right portion reveals the topmost layer of the C_{60} honeycomb array. The height difference between those two layers was approximately 0.5 nm, indicating that the difference corresponds to the thickness of one C_{60} molecular layer, not to the atomic height of Au. The height difference is consistent with that obtained at the C_{60} array on a zinc porphyrin derivative-modified Ag(100) surface (0.44 nm) reported by Bonifazi et al.[9a] We also obtained a corrugation height of 0.35 nm for open-cage C_{60} derivative arrays formed on the ZnOEP-modified Au(100)−(hex) surface in our previous study.[20d] The electronic state, that is, the corrugation height of each C_{60} molecule in the topmost layer, must be influenced by the underlying coronene layer in the present case. Compared to the position of each C_{60} molecule between the two layers, each C_{60} molecule in the topmost layer is located at the same position as in the lower layer (see the schematic illustration in Figure 4). The C_{60} honeycomb array is assumed to be composed of multiple sets of two C_{60} spots. The intermolecular distance between the nearest-neighbor C_{60} molecules was measured to be 1.25 ± 0.07 nm, which is similar to the intermolecular distance of the coronene (4 × 4) adlayer on Au(111),[25,35] whereas the distance between the nearest-neighbor cavities (dark areas) consisting of C_{60} molecules was found to be 1.8−2.1 nm in the honeycomb array. It is assumed that the honeycomb array is partially distorted. Remarkably, a careful inspection of the STM image revealed that the internal structure of each C_{60} molecule is in the shape of a stripe even at room temperature. In general, each C_{60} molecule in the adlayer on Au(111) appears as a round spot because of its rotational motion. It was reported that the rotational movement of C_{60} on Au(111) and Au(110) was hindered, and hence, the electronic structure was observed as an internal structure at the low temperature of 4.5 K in UHV,[17a,36] whereas featureless round spots were observed at room temperature. According to a report by Kunitake and co-workers, the specific feature for the restricted rotational motion

(35) Seidel, C.; Ellerbrake, R.; Gross, L.; Fuchs, H. *Phys. Rev. B* **2001**, *64*, 195418.

(36) Behler, S.; Lang, H. P.; Pan, S. H.; Thommen-Geiser, V.; Guntherodt, H.-J. *Z. Phys. B: Condens. Matter* **1993**, *91*, 1.

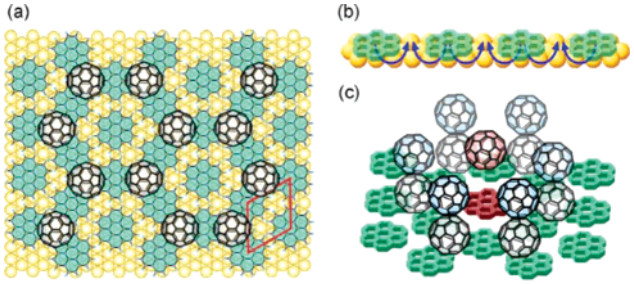

Figure 5. (a) Proposed model for the honeycomb array. (b) Schematic illustration of electron donation from coronene molecules to the Au substrate. (c) Schematic illustration of a trapped C_{60} molecule in the honeycomb cavity.

of C_{60} was observed on the iodine-modified Pt(111) surface in an acidic solution at room temperature, indicating that the interaction between the C_{60} molecule and an iodine-modified Pt(111) surface is much stronger than that between a C_{60} molecule and Au(111).[18c] In the system of C_{60} on the coronene-modified Au(111) surface, the adsorption of coronene on Au(111) might enhance the interaction between C_{60} and the Au substrate, suggesting that the coronene adlayer plays a significant role in the interaction between C_{60} and Au(111).

A prolonged immersion time, for example, 15 s, provided several C_{60} molecules trapped in cavities of the honeycomb array as the topmost layer (see Figure 4e and f). This phenomenon was observed when the third layer was formed. From the STM image shown in Figure 4f, the intermolecular spacing between the nearest-neighbor brightest spots was measured to be 1.8−2.0 nm, which is consistent with the spacing between dark cavities consisting of C_{60} molecules. The difference in height between the brightest and the less bright spots was approximately 0.20 nm. Furthermore, the number of C_{60} molecules trapped in the cavities increased upon immersion for a longer period of time. As can be seen in Figure 4g and h, the trapped C_{60} molecules in the honeycomb cavities were triangular in shape. Although the STM image was strongly dependent upon bias and tunneling conditions, the result of Figure 4h suggests that these cavities consisting of six C_{60} molecules provide a specific electronic situation or that the trapped C_{60} molecule does not attach to the bottom lowest coronene molecule, that is, the central C_{60} molecule stands out in the cavities of the honeycomb array. Note that no organized arrays were found on the coronene-modified Au(111) surface when the modification was carried out for the open-cage C_{60} derivative (see Figure S1), suggesting that the assembly of fullerene molecules on the coronene-modified Au(111) surface is influenced by the symmetry of the fullerene molecules.

On the basis of the STM images shown in Figure 4, the formation of a honeycomb array can be explained tentatively by the following model. The intermolecular distance of C_{60} indicates that each C_{60} molecule is located on a 3-fold site of the (4×4) coronene adlayer, where bare Au atoms are exposed, as shown in Figure 5a. When each C_{60} molecule is positioned on a 3-fold site, the resulting structure calls for the location of one coronene molecule at the center of a hexagon consisting of six C_{60} molecules. The C_{60} molecules might adsorb preferentially on a bare Au site rather than on top of coronene because the adsorption energy of C_{60} on Au(111) is high, which is estimated to be 40−60 kcal mol^{-1}.[37] In addition, as was mentioned in the section on the coronene adlayer, the charge distribution on exposed Au sites might be locally enhanced by the adsorption

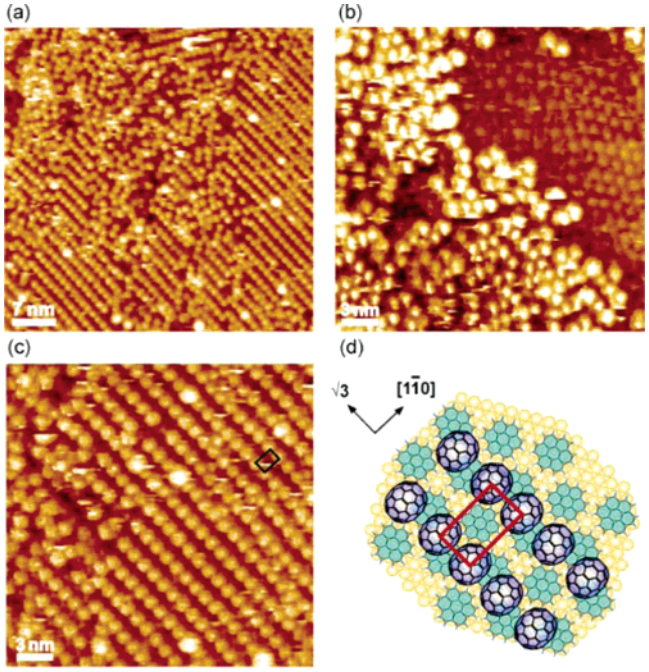

Figure 6. (a) Typical large-scale (50×50 nm^2) and (b,c) high-resolution (25×25 nm^2) STM images, obtained at 0.85 V versus RHE, of C_{70} arrays on highly ordered coronene-modified Au(111) in 0.1 M $HClO_4$. The potential of the tip and the tunneling current were 0.45 V and 0.31 nA, respectively. (d) Structural model of the topmost layer of the C_{70} arrays on the coronene-modified Au(111) surface.

of coronene because of the π-electron donating ability of coronene, as shown in Figure 5b. On the contrary, because the molecule of C_{60} has a strong electron accepting ability, it favors the Au site surrounded by three coronene molecules. As indicated by the results of investigations using high-resolution electron energy loss spectroscopy (HREELS)[38] and ultraviolet photoelectron spectroscopy (UPS)[38] in UHV, the C_{60} adlayer on Au(111) undergoes charge transfer from the Au surface to the adsorbed C_{60} molecules. According to Tzeng et al., the amount of transferred charge estimated from photoemission was 0.8 electron per C_{60} molecule on Au(111),[39] suggesting the possibility of strong π-electron donation from the Au surface to C_{60}. Thus, coronene molecules, especially the central coronene molecule surrounded by six C_{60} molecules, apparently play a role in the repulsion of the adsorption of C_{60}, as illustrated in Figure 5c.

For the C_{70} adlayer prepared in the same manner, the STM image was entirely different from that of the C_{60} arrays, as shown in Figure 6a, which is a typical large-scale STM image of a C_{70} adlayer on the coronene-modified Au(111) surface. Several one-dimensionally (1D) ordered arrays consisting of bright spots were present in the adlayer, whereas a disordered phase was seen in the middle portion of Figure 6a. A small rotational domain of ordered C_{70} molecules was seen in the upper portion of Figure 6a. Also, an area not covered with C_{70} was found, as shown in Figure 6b. In view of the molecular directions of both the coronene and C_{70} arrays, it is evident that the 1D array of the C_{70} molecules is aligned in the $\sqrt{3}$ direction

(37) Pérez-Jiménez, Á. J.; Palacios, J. J.; Louis, E.; SanFabián, E.; Vergés, J. A. *ChemPhysChem* **2003**, *4*, 388.
(38) Modesti, S.; Cerasari, S.; Rudolf, P. *Phys. Rev. Lett.* **1993**, *71*, 2469.
(39) Tzeng, C.-T.; Lo, W.-S.; Yuh, J.-Y.; Chu, R.-Y.; Tsuei, K.-D. *Phys. Rev. B* **2000**, *61*, 2263.

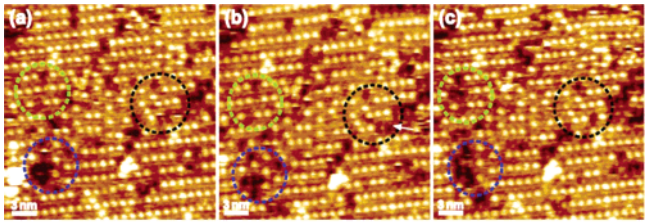

Figure 7. Time-dependent, high-resolution (25×25 nm^2) STM images of C_{70} arrays on a coronene-modified Au(111) surface acquired at 0.10 V versus RHE in 0.1 M $HClO_4$. The potential of the tip and the tunneling current were 0.35 V and 0.30 nA, respectively.

of the underlying coronene layer or the Au(111) substrate. A high-resolution STM image of the 1D-ordered C_{70} adlayer formed on the coronene-modified Au(111) surface is shown in Figure 6c. On the basis of the cross-sectional profile, the C_{70} array with a nearest-neighbor spacing of 1.05 nm is seen to be aligned in the $\sqrt{3}$ direction, whereas the intermolecular distance between bright spots in the $[1\bar{1}0]$ Au lattice direction was found to be 1.7−1.8 nm. The height amplitude was approximately 0.2 nm. As was mentioned in the section on C_{60}, the coronene adlayer on Au(111) is slightly changed in structure during the modification of the C_{60} molecules. Therefore, a similar distortion of the C_{70} array on the coronene-modified Au(111) surface is expected to occur during the formation of the C_{70} array. Although the exact relationship between the (4×4) coronene array and the C_{70} array could not be determined, a structural model illustrated in Figure 6d is proposed tentatively for the C_{70} adlayers on the coronene-modified Au(111), in which the unit cell is based on a $(6 \times 2\sqrt{3})$*rect* structure. In this case, each C_{70} molecule is assumed to be aligned to the $\sqrt{3}$ direction with a "lying-down" orientation, that is, the long-axis side of the C_{70} molecule is attached on the 2-fold bridge site of the (4×4) coronene array, because the lengths of the short and long axes of the C_{70} molecule were estimated to be 0.90 and 1.20 nm, respectively.[9c] Note that the 1D C_{70} arrays were strongly influenced by the modification condition. Under the conditions of a high concentration or a long immersion time, randomly or hexagonally arranged C_{70} adlayers were formed. The 1D C_{70} array, therefore, possesses a metastable adlayer structure.

When a very different scanning condition was used, a structural change involving an exchange of the C_{70} positions took place in the 1D-ordered C_{70} adlayer, which was caused by the scanning tip. Such a phenomenon was often observed in a slightly disordered domain during a continuous scan. For example, the defects in the molecular rows were observed to undergo exchange reactions under the bias voltage of 0.25 V and the current of 0.30 nA, as shown in Figure 7. The STM images were recorded with an interval of 1 min, which show weak bright spots between bright molecular rows. It is difficult to judge whether underlying coronene molecules existed or not. Judging from the depth between the brightest and the darkest parts (ca. 0.5 nm), it is possible that the brightest molecular rows compose the second layer of the C_{70} molecules formed on the 1D-ordered C_{70} arrays. The regions indicated by dotted circles in Figure 7a−c show the corresponding area. Especially the dark spot indicated by the white arrow near the black dotted circle in Figure 7b changed to a bright spot after 1 min, that is, the new bright spot appeared as seen in Figure 7c. The exchange reactions of bright spots in the C_{70} adlayer in the regions marked by green and blue dotted circles were also found to proceed

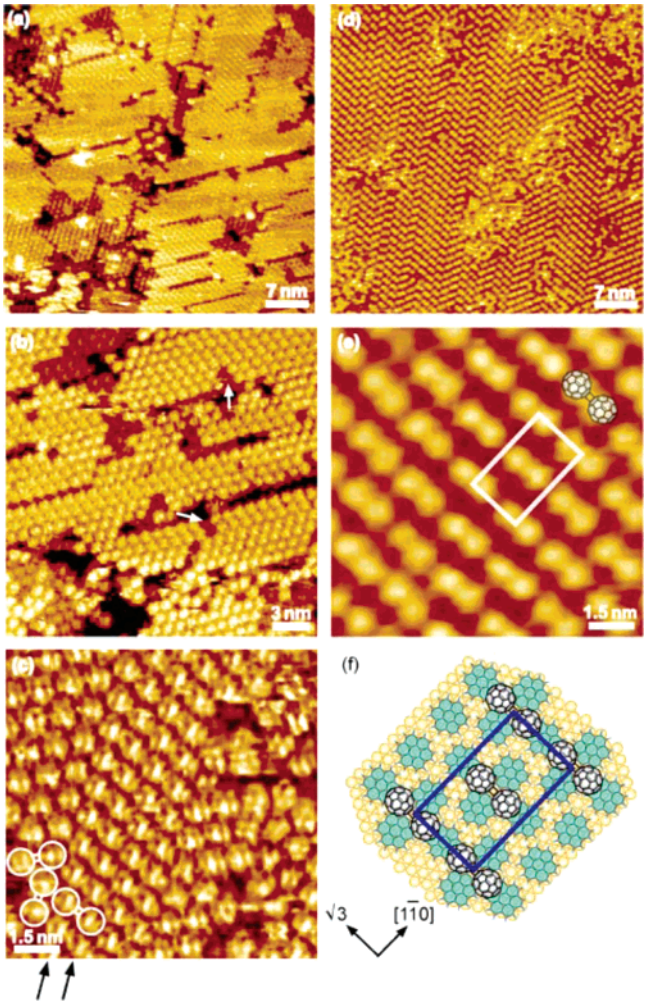

Figure 8. Typical STM images of C_{120} arrays formed on (a−c) clean Au(111) and (d,e) coronene-modified Au(111) surfaces, both recorded at 0.85 V versus RHE in 0.1 M $HClO_4$. The substrate was immersed into a C_{120}-saturated benzene solution for 3 min. The potential of the tip was 0.45 V versus RHE. The tunneling currents were (a) 0.50, (b) 0.30, (c) 1.00, (d) 0.50, and (e) 0.50 nA. (f) Proposed model of the topmost layer of the C_{120} array on the coronene adlayer on Au(111).

with an increase in elapsed time. The C_{70} array on the coronene-modified Au(111) surface was stably observed in the potential range between 0.05 and 0.80 V. However, when the bias voltage was set at a value lower than 0.20 V, the 1D-ordered C_{70} array gradually became disordered as the tip continued to be scanned. The honeycomb-like structure was formed with a continuous scan (see Figure S2).

C_{120} and C_{130} Dimer Arrays. To extend and explore the possibility of epitaxial growth, further investigations were performed for the adlayers of the [2 + 2]-type fullerene homodimer C_{120} and heterodimer C_{130} on both clean and coronene-modified Au(111) surfaces. When the modification of C_{120} was carried out for 3 min, a multilayer of C_{120} molecules was formed on Au(111). Figure 8a shows a typical large-scale STM image of a C_{120} adlayer observed at 0.80 V (near OCP) on Au(111) in 0.1 M $HClO_4$. The terrace was covered with epitaxial layers of C_{120} molecules. In the STM image of Figure 8a, three layers of C_{120} can be recognized. Molecular rows of the topmost layer crossed each other at an angle of approximately 60°. Especially the multilayer (at least the bilayer) of C_{120} formed on Au(111) shows a much clearer internal

structure, as shown in Figure 8b. Even in the close-packed region, the molecular orientation of each C_{120} molecule is easily recognized with a bifurcated feature in each C_{60} cage, as reported in the paper on the investigation of the adlayer structure of C_{120} on Au(111) in UHV.[19b] It is suggested that the vertical interaction between C_{120} molecules in the adlayers is greatly increased by the epitaxial growth. Also, several defects were clearly seen in the topmost layer of the C_{120} molecules, as indicated by the white arrow signs in Figure 8b. Those defects reflect the fact that a set of two cages form one C_{120} molecule. A close-up view of the topmost layer is shown in Figure 8c. Each C_{120} molecule is clearly seen to have a dumbbell shape. The C_{60} cages in an individual C_{120} molecule were not simply round but possessed an internal structure, although C_{60} molecules are seen as round circles, as reported in the previous papers.[19] The observed features with the shape of stripes are very similar to those of C_{60} on the coronene-modified Au(111). For the C_{120} molecule, the rotational motion is also prohibited on the Au surface. A careful inspection of the STM image of Figure 8c reveals that the direction of the stripe patterns in each C_{60} cage is slightly distorted in the $\sqrt{3}$ direction, as indicated by the two arrows, whereas the stripe pattern was perpendicular to the axis of the dumbbell dimer. On the basis of the discussion presented previously in this paper, one C_{120} molecule can be viewed as superimposed white dumbbells consisting of two circles and a square drawn by the white solid line in Figure 8c. The adlattice of C_{120} molecules is assigned to the $(2\sqrt{3} \times 5\sqrt{3})$-*R*30° symmetry in the close-packed region, as reported in our previous papers.[19]

In contrast, when C_{120} molecules were adsorbed on the coronene-modified Au(111) surface, a different ordered array was formed. In the STM image of a large area of 50×50 nm^2 shown in Figure 8d, each individual molecule of C_{120} can be clearly recognized as a set of two bright spots. Also, several defects are clearly seen as elongated dark spots in the adlayer. The molecules are aligned in the same direction or cross each other at an angle of 60 or 120° (sometimes 30°). The packing arrangement of the C_{120} adlayer on the coronene-modified Au(111) is quite different from that of C_{120} directly attached to Au(111), as described in our previous paper.[19] A high-resolution STM image is shown in Figure 8e. Each C_{120} molecule can be seen as a set of two spots with the so-called dumbbell shape. It is clear that the long axis of all C_{120} molecules is oriented in the same direction, that is the $[1\bar{1}\bar{2}]$ ($\sqrt{3}$) direction. The molecular rows of C_{120} were rotated by 30° with respect to the direction of the atomic row of Au. The intermolecular distances between nearest-neighbor molecules aligned along the $[1\bar{1}0]$ and $[1\bar{1}\bar{2}]$ directions were measured to be 3.22 ± 0.10 and 2.03 ± 0.07 nm, respectively, corresponding to 11 and $4\sqrt{3}$ times the Au lattice constant. Therefore, the adlattice of C_{120} on the coronene-modified Au(111) surface is assigned as a $c(11 \times 4\sqrt{3})$*rect* structure with respect to the underlying Au lattice constant. On the coronene-modified Au(111) surface, the internal structure of each C_{120} molecule could not be observed, suggesting that the interaction between C_{120} molecules and coronene is entirely different from that between C_{120} and the Au substrate. A structural model of the highly ordered C_{120} array on the coronene-modified Au(111) surface is proposed in Figure 8f.

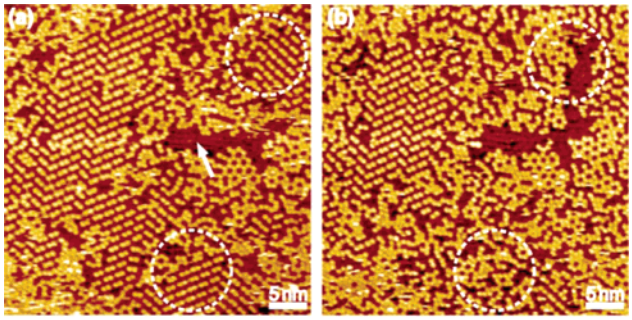

Figure 9. Typical STM images, acquired at 0.85 V versus RHE, of a C_{120} array on coronene-modified Au(111) in 0.1 M $HClO_4$. The potential of the tip was 0.45 V versus RHE. The tunneling currents were (a) 0.50 and (b) 0.30 nA.

From the molecular size and the adsorption site, the center of each C_{120} molecule is assumed to be located between coronene molecules.

Furthermore, the tunneling current dependence of the C_{120} topmost layer was carefully examined on the coronene-modified Au(111) surface. The C_{120} adlayer on the coronene-modified Au(111) was clearly seen at tunneling currents lower than 1.0 nA. However, the structure of the topmost layer of the C_{120} molecules was strongly influenced by tunneling currents higher than 1.5 nA with the tip potential of 0.45 V (bias voltage was 0.40 V). As shown in Figure 9, the C_{120} adlayer on the coronene-modified Au(111) surface transformed itself into a honeycomb-like structure during the scan of the tip. For example, the upper region of the highly ordered array of C_{120} molecules marked by the white dotted circle in Figure 9a was completely rearranged to form a honeycomb-like structure with some gaps, as can be seen in the region encircled by the white dotted line in Figure 9b. A careful inspection of the dark gap region revealed each coronene molecule in the underlying layer. This result indicates that the interaction between the C_{120} molecule and the coronene-modified Au(111) surface becomes much weaker than that between the C_{120} molecule and a clean Au(111) surface. Similar dependencies on tunneling current and bias voltage were found in the supramolecularly assembled fullerenes such as C_{60},[20a] open-cage C_{60},[20b,c] and ferrocene-linked C_{60} derivatives[20d] on the highly ordered ZnOEP array formed on both Au(111) and Au(100). It should be noted that the size of the honeycomb array consisting of C_{120} molecules was smaller than that obtained with C_{60} molecules.

For C_{130} adlayers, a slightly different mode of epitaxial growth was found on the clean Au(111) surface, whereas a similar adlayer was formed on the coronene-modified Au(111) surface. The STM image of Figure 10a shows that three layers were epitaxially formed on the terrace of the clean Au(111) surface. Each domain seems to be composed of hexagonally arranged bright spots. A typical high-resolution STM image of the C_{130} adlayer is shown in Figure 10b. The internal structure of individual C_{130} molecules is seen clearly in the topmost layer. As reported in our previous paper, a closely packed adlayer with an internal structure of individual C_{130} molecules was observed on Au(111) in UHV.[19b] The two bifurcated features of each set of two bright spots in the STM image, which are assigned to C_{60} and C_{70} cages, are not in parallel with each other, contrary to the case of the $C_{60}-C_{60}$ dumbbell dimer.[19b] A similar structure was observed for multilayers of C_{130} molecules on Au(111) even in aqueous solution. Figure 10c shows an STM image of a $C_{60}-$

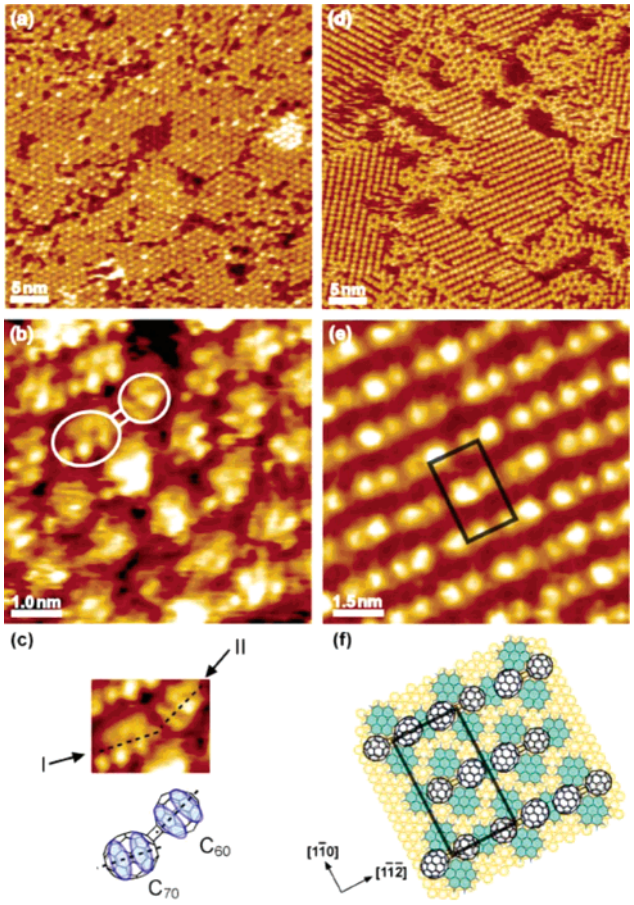

Figure 10. Typical large-scale (75 × 75 nm^2) and high-resolution (6 × 6 nm^2) STM images, obtained at (a) 0.85 V versus RHE and (b) 0.83 V, of C_{130} arrays on (a,b) a clean Au(111) surface and (d,e) on a coronene-modified Au(111) surface in 0.1 M $HClO_4$. The potentials of the tip and the tunneling currents were (a) 0.45 V versus RHE and 1.00 nA, (b) 0.42 V versus RHE and 1.70 nA, (d) 0.40 V versus RHE and 1.20 nA, and (e) 0.45 V versus RHE and 1.00 nA. (c) A clipped STM image and a model of a single C_{130} molecule. (f) A proposed model of the topmost layer of the C_{130} array on the coronene adlayer on Au(111).

C_{70} molecule clipped from Figure 10b and its structural model. Each set of two bright spots with several additional protrusions in the STM image, which are assigned to C_{60} and C_{70} cages, is not in parallel with each other (Figure 10b). This is understandable because, geometrically, the axes of the C_{60} and C_{70} cages in a $C_{60}-C_{70}$ molecule do not agree with each other, as seen in the model in Figure 10c, where the axes of the C_{70} and C_{60} cages are indicated by dashed lines I and II, respectively. For C_{70} molecules, the electronic structure has already been observed on Cu(111) by using STM.[40] It was reported that the bifurcated feature was perpendicular to the long axis of the C_{70} when the molecule was adsorbed on Cu(111) with its long axis parallel to the surface.[40] This bifurcated feature of C_{70} was also reproduced by a theoretical simulation.[40,41] Since the long axis of the C_{70} cage (line I) is tilted with respect to the bond axis of the C_{60} cage sharing the central cyclobutane ring (line II), as shown in the model in Figure 10c, it is expected that the bifurcated feature of C_{70} is not perpendicular to the bond axis. Apparently, line I is not along the bond axis, whereas line II penetrates the other cage in the $C_{60}-C_{70}$ molecules. On the basis of the discussion presented earlier in this paper, one C_{130} molecule can be assigned to two circles drawn in white on the STM image in Figure 10b. Thus, C_{130} molecules assemble on Au(111) with hexagonally arranged C_{60} and C_{70} cages in each C_{130} molecule to form a closely packed structure.

On the other hand, a flat C_{130} adlayer was formed on the coronene-modified Au(111) surface. In an area of 40 × 40 nm^2, three highly ordered rotational domains were found on the terrace, in which the long axis of each C_{130} molecule was aligned with that of the neighboring molecule. Several disordered phases were also seen between domains, which were similar to the honeycomb array, as shown in Figure 10d. The packing arrangement of the C_{130} array formed on the coronene-modified Au(111) surface was also different from that of C_{130} directly attached on Au(111).[19] The packing arrangement and the intermolecular distance of the C_{130} array were almost identical to those of the C_{120} array on the coronene-modified Au(111) surface. However, a more careful inspection revealed that there was a difference in brightness in the ordered C_{130} array. Although the orientation of each C_{130} molecule was compositionally disordered, that is, any regularity such as head-to-tail or head-to-head orientation was not found, it was possible to distinguish each C_{130} molecule as a pair of bright and brightest spots, as shown in Figure 10e. The intermolecular spacing between those bright spots was 0.90 nm, which corresponds to the intramolecular distance between the centers of the C_{60} and C_{70} cages. These spots are, thus, attributable to C_{60} and C_{70} cages in one C_{130} molecule, respectively, although no internal structure was observed under these conditions. The adlattice of C_{130} on the coronene-modified Au(111) surface was also assigned as a $c(11 \times 4\sqrt{3})$*rect* structure with respect to the underlying Au lattice constant, which is identical to that of the C_{120} array, as illustrated by the model shown in Figure 10f. However, in the case of the C_{130} array formed on the coronene-modified Au(111) surface, the adlayer structure was more strongly influenced by the conditions of the tunneling current and bias voltage. This is due to the unsymmetrical chemical structure of the C_{130} molecule. The highly ordered C_{130} array on the coronene-modified Au(111) surface easily changed into the honeycomb-like structure during several scans (see Figure S3), suggesting that the interaction between the C_{130} molecule and coronene-modified Au(111) becomes much weaker than that observed when the molecule is directly attached to the Au substrate. Note that $C_{60}-C-C_{70}$ (C_{131}) molecules formed a stable honeycomb-like array on the coronene-modified Au(111) surface.[42] The result shows that the insertion of one C atom between the C_{60} and C_{70} cages can alter the adsorption site of each cage. In all fullerenes arrays, similar structures were consistently observed in the potential range between 0.10 and 0.90 V.

C_{60} Triangular Trimer (C_{180}) Array. We further examined the triangular trimer (C_{180}) because C_{180} isomers have unique electronic and spectroscopic characteristics for electronic and photonic applications.[43] Unfortunately, the C_{180} adlayer directly attached to Au(111) was not highly ordered in our experimental conditions. The reason might be a contamination by, or the

(40) Wang, X.-D.; Yurov, V. Yu.; Hashizume, T.; Shinohara, H.; Sakurai, T. *Phys. Rev. B* **1994**, *49*, 14746.
(41) Maruyama, Y.; Ohno, K.; Kawazoe, Y. *Phys. Rev. B* **1995**, *52*, 2070.
(42) Zhao, Y.; Chen, Z.; Yuan, H.; Gao, X.; Qu, L.; Chai, Z.; Xing, G.; Yoshimoto, S.; Tsutsumi, E.; Itaya, K. *J. Am. Chem. Soc.* **2004**, *126*, 11134.
(43) Fujitsuka, M.; Fujiwara, K.; Murata, Y.; Uemura, S.; Kunitake, M.; Ito, O.; Komatsu, K. *Chem. Lett.* **2001**, 384.

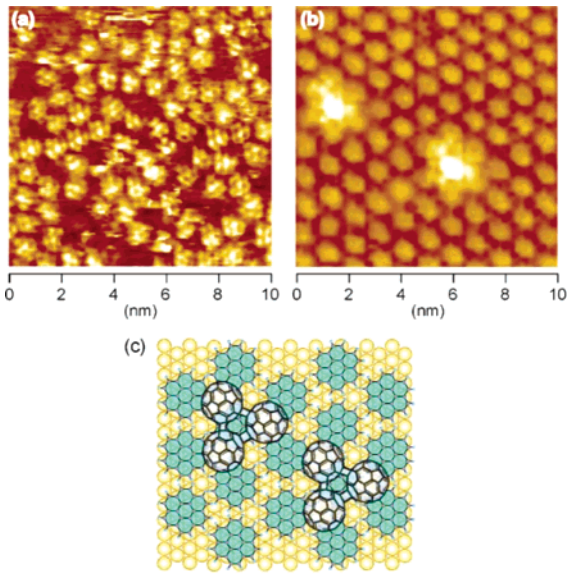

Figure 11. Typical high-resolution (10×10 nm^2) STM images of a C_{180} adlayer on (a) clean Au(111) and (b) coronene-modified Au(111) surfaces in 0.1 M $HClO_4$, acquired at (a) 0.80 V and (b) 0.85 V versus RHE. The potentials of the tip and the tunneling currents were (a) 0.40 V versus RHE and 3.00 nA and (b) 0.46 V versus RHE and 1.00 nA. (c) The proposed model of C_{180} molecules adsorbed on the coronene adlayer on Au(111).

inclusion of, other isomers.[18d] Actually, it is difficult to assign each C_{180} molecule to a C_{60} triangular trimer in Figure 11a. However, we could observe a clear internal structure. It appears to be different from the structure of the C_{120} or C_{130} adlayer on the clean Au(111) surface, suggesting that the rotational motion of each C_{60} cage is completely inhibited because of the sharing of the cyclobutane rings. In Figure 11a, a typical feature of the internal structure is the presence of three separated spots with several protrusions, not stripes. In contrast, the individual C_{180} molecule could be seen as the brightest central spot with three additional spots in the coronene adlayer, as can be seen in Figure 11b. Three C_{60} cages were positioned at the 3-fold site of coronene array (see Figure 11c). On the coronene adlayer, the C_{60} triangular trimer favors the adsorption on the hexagonal arrangement domain, that is, the triangular trimer can structurally match the coronene adlayer rather than other structural isomers. Therefore, the C_{60} triangular trimer might be selectively adsorbed on the coronene adlayer if other structural isomers are also present.

Conclusions

By successively immersing a Au(111) substrate into a benzene solution containing coronene and then into that containing fullerenes, we succeeded in forming supramolecularly assembled layers of fullerenes including C_{60}, C_{70}, a $C_{60}-C_{60}$ dumbbell dimer, a $C_{60}-C_{70}$ cross-dimer, and a C_{60} triangle trimer on the coronene-modified Au(111) surface. STM images clearly demonstrated details of not only the electrochemical structural change of the coronene adlayer but also the internal structure and packing arrangement of those fullerenes on a clean Au(111) surface and those of supramolecular assemblies on the coronene-modified Au(111) surface. Epitaxial growth of fullerenes on the Au(111) surface was found to be strongly influenced by the underlying coronene adlayer; thus, the control of adlayer structure is very important for the film formation. Especially the C_{60} assembly on the coronene-modified Au(111) surface provided a unique nanostructure of the honeycomb array. The trapping reaction of C_{60} molecules into cavities in the honeycomb array suggested the presence of a special electronic state. The adlayer structures of C_{70}, C_{120}, and C_{130} on the coronene-modified Au(111) surface strongly depended upon the condition of either the tunneling current or bias voltage, whereas the C_{60} honeycomb array was stable under the conditions of a higher tunneling current or bias voltage. Thus, the coronene adlayer plays an important role not only in the control of the donating ability of the Au surface but also in the selective recognition of the difference in shape and/or electronic structure of fullerenes. The findings of this study show that heterogeneous interfaces for donor−acceptor interaction can be built up based on the "bottom-up" strategy.

Acknowledgment. This work was supported, in part, by the Ministry of Education, Culture, Sports, Science and Technology, a Grant-in-Aid for Young Scientists (B) (No. 16750106/18750132) and the Center of Excellence (COE) Project, Giant Molecules and Complex Systems, 2006. The authors acknowledge the assistance provided by Dr. Y. Okinaka in writing this manuscript.

Supporting Information Available: STM image representing the structure of the entire surface modified with an open-cage C_{60} derivative on the coronene-modified Au(111) surface. Bias-dependent STM images of the C_{70} array on the coronene-modified Au(111) surface. Typical STM image of structural changes of the C_{130} array after several scans. This material is available free of charge via the Internet at http://pubs.acs.org.

JA0684848